

# Subtraction Procedure for Calculation of Anomalous Magnetic Moment of Electron in QED and its Application to Numerical Computation at 3-loop Level

S. A. Volkov

*SINP MSU, Moscow, Russia*

A new subtraction procedure for removal both ultraviolet and infrared divergences in Feynman integrals is proposed. This method is developed for computation of QED corrections to the electron anomalous magnetic moment. The procedure is formulated in the form of a forest formula with linear operators that are applied to Feynman amplitudes of UV-divergent subgraphs. The contribution of each Feynman graph that contains propagators of electrons and photons is represented as a finite Feynman-parametric integral. Application of the developed method to the calculation of 2-loop and 3-loop contributions is described.

## 1 Introduction

The Bogoliubov-Parasiuk theorem [1, 2] provides us a constructive definition of the procedure (R-operation) that removes all ultraviolet divergences in each Feynman graph. The proof of this theorem in [1, 2] gives the representation of the Feynman amplitude that is obtained by R-operation in the form of an absolutely convergent Schwinger-parametric integral if the imaginary addition  $i\varepsilon$  ( $\varepsilon > 0$ ) to the propagator denominators is fixed. Thus, R-operation removes UV-divergences point-by-point, before integration. The explicit formula for R-operation was obtained in [3, 4]:

$$\mathcal{R} = (1 - M_1)(1 - M_2) \dots (1 - M_n), \quad (1)$$

where  $M_j$  is the operator that extracts Taylor expansion of the Feynman amplitude of  $j$ -th divergent subgraph up to the needed order around zero momenta. Here it is meant that we should remove brackets and delete all terms containing  $M_j$  and  $M_l$  that correspond to overlapping<sup>1</sup> subgraphs. In

---

<sup>1</sup>Subgraphs are said to overlap if their sets of lines have non-empty intersection, and they are not contained one inside the other.

the same papers it was pointed out that this renormalized Feynman amplitude can be represented in the form of an absolutely convergent Schwinger-parametric integral when  $\varepsilon > 0$  is fixed. Later, this formula was independently rediscovered by Zimmermann in momentum representation [5], see also [41, 42].

Note that R-operation doesn't remove infrared divergences. For example, in QED, if we consider external momenta in Feynman graphs on the mass shell, then the Feynman amplitude that is renormalized by R-operation doesn't converge to a distribution as  $\varepsilon \rightarrow 0$ . Also, the physical renormalization requires to take the on-shell renormalization operators instead of  $M_j$  in (1), and these operators generate additional IR-divergences (see [6, 7]).

In this paper we consider a development of the R-operation idea. This development is applied to the problem of calculation of QED corrections to the electron's anomalous magnetic moment (AMM).

Electron's AMM is known with a very high accuracy, in the experiment [8] the value

$$a_e = 0.00115965218073(28)$$

(in Dirac moment units) was obtained. So, a maximal possible precision is needed also from theoretical predictions. For high-precision calculations it is required to take into account Feynman graphs with a large number of independent loops, this requires a lot of computer resources. Therefore, the ability to remove all divergences (including the infrared ones) point-by-point is certainly relevant. Generally speaking, electron's AMM in QED is free from infrared divergences in each order of the perturbation series since IR-divergences of the unrenormalized Feynman amplitude are cancelled by IR-divergences in renormalization constants (about IR-divergences in renormalization constants, see [6, 7]). However, individual graphs remain IR-divergent. Unfortunately, the structure of infrared and ultraviolet divergences in individual graphs is complicated, the divergences of different types can, in a certain sense, be "entangled" with each other. At the given moment, there is no any universal method for subtraction of IR-divergences in QED Feynman graphs.

The most accurate prediction of electron's AMM at the present moment [9, 10] has the following representation:

$$a_e = a_e(\text{QED}) + a_e(\text{hadronic}) + a_e(\text{electroweak}),$$

$$a_e(\text{QED}) = \sum_{n \geq 1} \left(\frac{\alpha}{\pi}\right)^n a_e^{2n},$$

$$a_e^{2n} = A_1^{(2n)} + A_2^{(2n)}(m_e/m_\mu) + A_2^{(2n)}(m_e/m_\tau) + A_3^{(2n)}(m_e/m_\mu, m_e/m_\tau),$$

where  $m_e$ ,  $m_\mu$ ,  $m_\tau$  are masses of electron, muon, and tau lepton, respectively. The value  $A_1^{(2)} = 0.5$  was obtained analytically by Schwinger in 1948 [11, 12]. The term  $A_1^{(4)}$  was first calculated by Karplus and Kroll [13] using combined numerical-analytical method but there was a mistake in that calculation. This mistake was corrected analytically by Petermann [14] and Sommerfield [15], the new value was confirmed by using another approach in [16]:

$$A_1^{(4)} = -0.328478965579193\dots \quad (2)$$

The value  $A_1^{(6)}$  was computed numerically with the help of computers by three groups of scientists in the first half of 1970s (see [17], [18, 19], [20]). The most accurate value  $A_1^{(6)} = 1.195 \pm 0.026$  for that period of time was obtained by Kinoshita and Cvitanović [20] (the error is due to the Monte Carlo integration). By 1995, the accuracy was improved [21]:  $A_1^{(6)} = 1.181259(40)$ . In all three cases, the base of the method was a subtraction procedure for point-by-point elimination of IR and UV divergences. These subtraction procedures were developed especially for 3-loop calculation of electron's AMM. However, in all three cases, a finite renormalization after the subtraction was required. The rules for this renormalization in the 3-loop case doesn't lead to an automated procedure at any order of perturbation. Simultaneously, approximately at the end of 1960s, the work of analytical calculation of  $A_1^{(6)}$  was started with help of computers (see [22–33] etc.). This work was finished in 1996 when in [33] the value

$$A_1^{(6)} = 1.181241456\dots \quad (3)$$

was obtained. The first numerical values for  $A_1^{(8)}$  were computed by Kinoshita and Lindquist at the beginning of 1980s (see [34]), since then the accuracy is still improving by Kinoshita and his collaborators. The numerical value for  $A_1^{(10)}$  was first obtained by Kinoshita's team in 2012 [9]. To realize that calculation, a new subtraction procedure for point-by-point removal of divergences was developed. The new method of Kinoshita and collaborators was fully automated up to  $A_1^{(8)}$ , however, some individual Feynman graphs for  $A_1^{(10)}$  require a special treatment [35]. In paper [10] the recent results of computation was presented:

$$A_1^{(8)} = -1.91298(84), \quad A_1^{(10)} = 7.795(336).$$

The corresponding theoretical prediction

$$a_e = 0.001159652181643(25)(23)(16)(763)$$

was obtained by using the value of the fine structure constant  $\alpha^{-1} = 137.035999049(90)$  that had been measured in the recent experiments with rubidium atoms (see [36, 37]). Here, the first, second, third, and fourth uncertainties come from  $A_1^{(8)}$ ,  $A_1^{(10)}$ ,  $a_e(\text{hadronic}) + a_e(\text{electroweak})$  and the fine-structure constant<sup>2</sup> respectively. Let us note that at the present moment there is no any independent check of the calculation of  $A_1^{(8)}$  and  $A_1^{(10)}$ , therefore, the problem of computing  $A_1^{(2n)}$  is still relevant. Some terms of the expansion of  $A_2^{(2n)}$  and  $A_3^{(2n)}$  ( $n \leq 4$ ) in powers of  $m_e/m_\mu$ ,  $m_e/m_\tau$ , logarithms of  $m_e/m_\mu$  and  $m_e/m_\tau$  are known analytically (see [38, 39]). Also, these values and  $A_2^{(10)}(m_e/m_\mu)$  were computed numerically (see [10]), and the results of this computation for  $A_2^{(2n)}$ ,  $A_3^{(2n)}$  ( $n \leq 4$ ) are in good agreement with the analytical ones.

In this paper we present a new subtraction procedure for calculation of  $A_1^{(2n)}$ . This procedure eliminates IR and UV divergences point-by-point, before integration, in the spirit of the papers [1–4, 41, 42, 9, 10, 17–20] etc. The method has the following advantages:

- The method is fully automated for any  $n$ .
- The method is comparatively easy for realization on computers.
- The given subtraction procedure is a modification of (1), it differs from that one only in the choice of operators and in the way of combining them. Operators of a simple form are used, which transform Feynman amplitudes of subgraphs. The operators can be cast in the momentum representation, they are linear, and produce polynomials of the degree that is less or equal to the ultraviolet degree of divergence of the corresponding subgraph<sup>3</sup>.
- The contribution of each Feynman graph to  $A_1^{(2n)}$  can be represented as a single Feynman-parametric integral. The value of  $A_1^{(2n)}$  is a sum of these contributions. So, we don't need any additional finite renormalizations, calculations of renormalization constants, calculations of some values at the lower orders of perturbation, or other additional calculations.
- The given subtraction procedure was checked for 2-loop and 3-loop Feynman graphs by numerical integration. Most likely, it will work at

---

<sup>2</sup>Thus, the computed coefficients are used for improving the accuracy of  $\alpha$ .

<sup>3</sup>The subtraction procedures in [9, 17–20] use the operators that work with formulas in Feynman-parametric or momenta representation (not with functions).

the higher orders of perturbation (the detailed explanation will be given elsewhere [40]).

- It is possible to use Feynman parameters directly. We don't need any additional tricks<sup>4</sup> to define Feynman parameters in Feynman graphs that have non-negative UV degrees of divergence.

Presumably, the ideas of the given method can be applied to some other problems.

## 2 Formulation of the method

### 2.1 Preliminary remarks

We will work in the system of units, in which  $\hbar = c = 1$ , the factors of  $4\pi$  appear in the fine-structure constant:  $\alpha = e^2/(4\pi)$ , the tensor  $g_{\mu\nu}$  is defined by

$$g_{\mu\nu} = g^{\mu\nu} = \begin{pmatrix} 1 & 0 & 0 & 0 \\ 0 & -1 & 0 & 0 \\ 0 & 0 & -1 & 0 \\ 0 & 0 & 0 & -1 \end{pmatrix},$$

the Dirac gamma-matrices satisfy the following condition  $\gamma^\mu\gamma^\nu + \gamma^\nu\gamma^\mu = 2g^{\mu\nu}$ .

We will use Feynman graphs with propagators  $\frac{i(\hat{p}+m)}{p^2-m^2+i\varepsilon}$  for electron lines and

$$\frac{-g_{\mu\nu}}{p^2+i\varepsilon} \tag{4}$$

for photon lines. It is always assumed that a Feynman graph is strongly connected and doesn't have odd electron cycles.

The number  $\omega(G) = 4 - N_\gamma - \frac{3}{2}N_e$  is called the *ultraviolet degree of divergence* of the graph  $G$ . Here,  $N_\gamma$  is the number of external photon lines of  $G$ ,  $N_e$  is the number of external electron lines of  $G$ .

If for some subgraph<sup>5</sup>  $G'$  of the graph  $G$  the inequality  $\omega(G') \geq 0$  is satisfied, then UV-divergence can appear. A graph  $G'$  is called UV-divergent if  $\omega(G') \geq 0$ . There are the following types of UV-divergent subgraphs in QED Feynman graphs: *electron self-energy subgraphs* ( $N_e = 2, N_\gamma = 0$ ),

---

<sup>4</sup>For example, one can use  $m^2$  in propagators as additional variables of integration (see [43, 20]).

<sup>5</sup>In this paper we consider only such subgraphs that are strongly connected and contain all lines that join the vertexes of the given subgraph.

photon self-energy subgraphs ( $N_e = 0, N_\gamma = 2$ ), vertex-like subgraphs ( $N_e = 2, N_\gamma = 1$ ), photon-photon scattering subgraphs<sup>6</sup> ( $N_e = 0, N_\gamma = 4$ ).

## 2.2 Anomalous magnetic moment in terms of Feynman amplitudes

A set of subgraphs of a graph is called a *forest* if any two elements of this set are not overlapped.

For vertex-like graph  $G$  by  $\mathfrak{F}[G]$  we denote the set of all forests  $F$  containing UV-divergent subgraphs of  $G$  and satisfying the condition  $G \in F$ . By  $\mathfrak{I}[G]$  we denote the set of all vertex-like subgraphs  $G'$  of  $G$  such that each  $G'$  contains the vertex that is incident<sup>7</sup> to the external photon line of  $G$ .<sup>8</sup>

Let us define the following linear operators that are applied to the Feynman amplitudes of UV-divergent subgraphs:

1.  $A$  — projector of the anomalous magnetic moment. This operator is applied to the Feynman amplitudes of vertex-like subgraphs. Let  $\Gamma_\mu(p, q)$  be the Feynman amplitude corresponding to an electron of initial and final four-momenta  $p - q/2$ ,  $p + q/2$ . The Feynman amplitude  $\Gamma_\mu$  can be expressed in terms of three form-factors:

$$\bar{u}_2 \Gamma_\mu(p, q) u_1 = \bar{u}_2 \left( f(q^2) \gamma_\mu - \frac{1}{2m} g(q^2) \sigma_{\mu\nu} q^\nu + h(q^2) q_\mu \right) u_1,$$

where  $(p - q/2)^2 = (p + q/2)^2 = m^2$ ,  $(\hat{p} - \hat{q}/2 - m)u_1 = \bar{u}_2(\hat{p} + \hat{q}/2 - m) = 0$ ,

$$\sigma_{\mu\nu} = \frac{1}{2}(\gamma_\mu \gamma_\nu - \gamma_\nu \gamma_\mu),$$

see, for example, [6]. By definition, put

$$A\Gamma_\mu = \gamma_\mu \cdot \lim_{q^2 \rightarrow 0} (g(q^2) + C_A h(q^2)), \quad (5)$$

where  $C_A$  is an arbitrary constant (the final result doesn't depend on  $C_A$ , but contributions of individual Feynman graphs can depend).

2. The definition of the operator  $U$  depends on the type of UV-divergent subgraph to which the operator is applied:

---

<sup>6</sup>The divergences of this type are cancelled in the sum of all Feynman graphs, but they can appear in individual graphs.

<sup>7</sup>We say that a vertex  $v$  and a line  $l$  are *incident* if  $v$  is one of endpoints of  $l$ .

<sup>8</sup>In particular,  $G \in \mathfrak{I}[G]$ .

- If  $\Pi$  is the Feynman amplitude that corresponds to a photon self-energy subgraph or a photon-photon scattering subgraph, then, by definition,  $U\Pi$  is a Taylor expansion of  $\Pi$  around zero momenta up to the UV divergence degree of this subgraph.
- If  $\Sigma(p)$  is the Feynman amplitude that corresponds to an electron self-energy subgraph,

$$\Sigma(p) = a(p^2) + b(p^2)\hat{p}, \quad (6)$$

then, by definition<sup>9</sup>,

$$U\Sigma(p) = a(m^2) + b(m^2)\hat{p}.$$

- If  $\Gamma_\mu(p, q)$  is the Feynman amplitude that corresponds to vertex-like subgraph,

$$\Gamma_\mu(p, 0) = a(p^2)\gamma_\mu + b(p^2)p_\mu + c(p^2)\hat{p}p_\mu + d(p^2)(\hat{p}\gamma_\mu - \gamma_\mu\hat{p}), \quad (7)$$

then, by definition,

$$U\Gamma_\mu = (a(m^2) + C_U d(m^2))\gamma_\mu, \quad (8)$$

where  $C_U$  is an arbitrary constant.

3.  $L$  is the operator that is used for on-shell renormalization of vertex-like subgraphs. If  $\Gamma_\mu(p, q)$  is the Feynman amplitude that corresponds to a vertex-like subgraph,

$$\Gamma_\mu(p, 0) = a(p^2)\gamma_\mu + b(p^2)p_\mu + c(p^2)\hat{p}p_\mu + d(p^2)(\hat{p}\gamma_\mu - \gamma_\mu\hat{p}),$$

then, by definition,

$$L\Gamma_\mu = [a(m^2) + mb(m^2) + m^2 c(m^2)]\gamma_\mu. \quad (9)$$

Let  $f_G$  be the unrenormalized Feynman amplitude that corresponds to a vertex-like graph  $G$ . By definition, put

$$\tilde{f}_G = \mathcal{R}_G^{new} f_G, \quad (10)$$

where

$$\mathcal{R}_G^{new} = \sum_{\substack{F=\{G_1, \dots, G_n\} \in \mathfrak{S}[G] \\ G' \in \mathfrak{J}[G] \cap F}} (-1)^{n-1} M_{G_1}^{F, G'} M_{G_2}^{F, G'} \dots M_{G_n}^{F, G'}, \quad (11)$$

---

<sup>9</sup>Note that it differs from the standard on-shell renormalization.

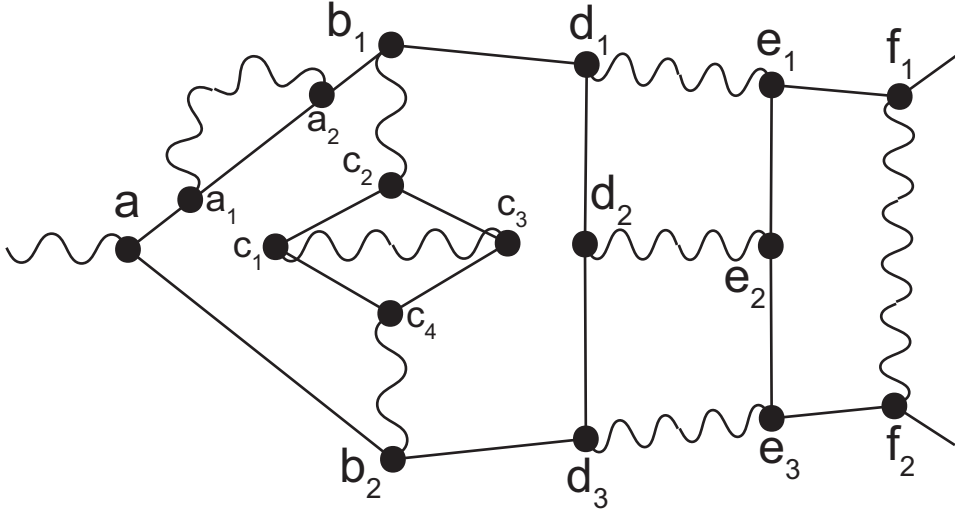


Figure 1: A complicated Feynman graph (an example)

$$M_{G''}^{F,G'} = \begin{cases} A_{G'}, & \text{if } G' = G'', \\ U_{G''}, & \text{if } G'' \notin \mathfrak{J}[G] \text{ or } G'' \subseteq G', G'' \neq G', \\ L_{G''}, & \text{if } G'' \in \mathfrak{J}[G], G' \subseteq G'', G'' \neq G, G'' \neq G', \\ (L_{G''} - U_{G''}), & \text{if } G'' = G, G' \neq G. \end{cases} \quad (12)$$

In this notation, the subscript of a given operator symbol denotes the subgraph to which this operator is applied.

By  $\check{f}_G$  we denote the coefficient before  $\gamma_\mu$  in  $\check{f}_G$ . The value  $\check{f}_G$  is the contribution of graph  $G$  to the anomalous magnetic moment:

$$a_{e,1}^{new} = \sum_G \check{f}_G,$$

where the summation goes over all vertex-like Feynman graphs. If we sum only over graphs with a fixed number of vertices, we can obtain the corresponding term of the perturbation expansion in  $\alpha$ .

Let us consider the example that is showed on Figure 1. This Feynman graph we denote by  $G$ . For this example, we have

$$\mathfrak{J}[G] = \{G_c, G_e, G\},$$

where

$$G_c = aa_1a_2b_1b_2c_1c_2c_3c_4, \quad G_e = aa_1a_2b_1b_2c_1c_2c_3c_4d_1d_2d_3e_1e_2e_3$$



(subgraphs are specified by enumeration of vertices). Also, there are following UV-divergent subgraphs:  $a_1a_2$  (electron self-energy),  $c_1c_2c_3$ ,  $c_1c_3c_4$  (vertex-like, overlapping),  $c_1c_2c_3c_4$  (photon self-energy),  $G_d = aa_1a_2b_1b_2c_1c_2c_3c_4d_1d_2d_3$  (photon-photon scattering). Using (10), (11), (12) we obtain

$$\begin{aligned}\tilde{f}_G &= [A_G(1 - U_{G_e})(1 - U_{G_d})(1 - U_{G_c}) - (L_G - U_G)A_{G_e}(1 - U_{G_d})(1 - U_{G_c}) \\ &\quad - (L_G - U_G)(1 - L_{G_e})(1 - U_{G_d})A_{G_c}] \\ &\quad \times (1 - U_{c_1c_2c_3c_4})(1 - U_{c_1c_2c_3} - U_{c_1c_3c_4})(1 - U_{a_1a_2})f_G.\end{aligned}$$

Operator expressions for 2-loop Feynman graphs are given in Table 2 (in this table by  $G$  we denote the whole graph).

### 2.3 Feynman-parametric representation

Let us consider the formulation of the subtraction procedure in Feynman-parametric representation. This representation allows to remove regularization, so it can be directly used for numerical calculation.

We will use the following formula:

$$\frac{1}{x + i\varepsilon} = \frac{1}{i} \int_0^{+\infty} e^{iz(x+i\varepsilon)} dz.$$

To calculate the contribution of vertex-like graph  $G$  to  $a_{e,1}^{new}$  in terms of Feynman parameters we should perform the following steps:

1. To each internal line of  $G$  we assign the variable  $z_j$ , where  $j$  is the number of this line.
2. Suppose that the values  $z_j > 0$  are fixed. We introduce the following propagators for electron and photon lines respectively:

$$(\hat{p} + m)e^{iz_j(p^2 - m^2 + i\varepsilon)}, \quad ig_{\mu\nu}e^{iz_j(p^2 + i\varepsilon)}. \quad (13)$$

By  $\check{f}_G(\underline{z}, \varepsilon)$ , where  $\underline{z} = (z_1, z_2, \dots)$ , we denote the value that is obtained by the rules that are described above for  $\check{f}_G$ , but with the use of the new propagators. The value  $\check{f}_G(\underline{z}, \varepsilon)$  is obtained by using explicit formulas for integrals of multi-dimensional gaussian functions multiplied by polynomials, see [41, 42]. After applying these explicit formulas to a Feynman integral with propagators (13) we obtain the Feynman amplitude of the form

$$\Pi_1 R_1 + \Pi_2 R_2 + \dots + \Pi_N R_N, \quad (14)$$

where each  $\Pi_l$  can be represented as a product of expressions like  $\hat{p}_j$ ,  $p_{j\mu}$ ,  $\gamma_\mu$ ,  $(p_{j'}p_{j''})$  (here  $p_1, p_2, \dots$  are momenta of external lines,  $j, j', j''$  are coordinate indexes of external momenta,  $\mu$  is the tensor index that corresponds to the external photon line), each  $R_l$  has the form

$$\frac{F(\underline{z})}{T(\underline{z})} \cdot \exp \left[ i \frac{H(\underline{p}, \underline{z})}{T(\underline{z})} - \varepsilon \sum z_j \right],$$

where  $\underline{p} = (p_1, p_2, \dots)$  is the tuple of external momenta,  $F, T, H$  are homogeneous polynomials with respect to  $z$ , all coefficients of the polynomial  $T$  are positive, all coefficients of  $H$  are real, the degree of  $H$  with respect to  $z$  is equal to 1 plus the degree of  $T$ , the polynomial  $H$  contains elements of  $\underline{p}$  only in the form of scalar products like  $(p_{j'}p_{j''})$ , and each term of  $H$  contains not more than one such scalar product (see [41, 42, 7]).

If operators  $A, U$ , and  $L$  are applied to some subgraphs of a given Feynman graph, then the corresponding Feynman amplitude can be represented in the form (14) too. This can be proved by induction on the number of internal lines using the following statements:

- The product of expressions like (14) that depend on non-intersecting subsets of  $\{z_1, \dots, z_n\}$  can be represented in the form (14) too.
- Operators  $A, U$ , and  $L$  give polynomials of external momenta.
- If  $\Phi$  is an expression of the form (14), then  $A\Phi, U\Phi, L\Phi$  can be represented in the form (14) too. For example,

$$A[\Pi_1 R_1 + \dots + \Pi_N R_N] = R_1 A\Pi_1 + \dots + R_N A\Pi_N. \quad (15)$$

This follows from the fact that  $A\Gamma_\mu(p, q)$  can be expressed through the values of  $\Gamma_\mu(p, q)$  on the surface  $p^2 = m^2, q = 0$  and its first derivatives at these points along directions  $(p', q')$  such that  $pp' = pq' = 0$  (see the explicit formula in [45]). The first derivatives of  $R_j$  at these points along these directions is equal to 0 because of zero first derivatives of scalar products of the external momenta.

3. By definition, put

$$I(z_1, \dots, z_n) = \lim_{\varepsilon \rightarrow +0} \int_0^{+\infty} \lambda^{n-1} \check{f}_G(z_1\lambda, \dots, z_n\lambda, \varepsilon) d\lambda. \quad (16)$$

The problem is reduced to the calculation of the integral

$$\int_{z_1, \dots, z_n > 0} I(z_1, \dots, z_n) \delta(z_1 + \dots + z_n - 1) dz_1 \dots dz_n. \quad (17)$$

The integral (16) is obtained analytically by using the formula

$$\int_0^{+\infty} \lambda^{D-1} e^{\lambda(ik-\varepsilon)} d\lambda = \frac{(D-1)!}{(\varepsilon - ik)^D}.$$

Note that we will always have  $D > 0$ . This follows from the fact that the terms with  $D = 0$  are nulled by the operator  $A$  that is applied to some subgraph. This is because the term in Feynman amplitude corresponding to the minimal  $D$  is proportional to  $\gamma_\mu$  (see the explicit recipe for constructing  $F$ ,  $G$ ,  $H$  in [43, 41, 42]).

4. We compute the integral (17) numerically.

### 3 Justification of the method

Justification of the correctness of the described subtraction procedure consists of two parts:

1. Proof of the equality  $a_{e,1}^{new} = a_{e,1}$ , where  $a_{e,1} = \sum_{n \geq 1} \left(\frac{\alpha}{\pi}\right)^n A_1^{(2n)}$ .
2. Demonstration that the subtraction procedure removes all divergences in each Feynman graph.

Let us consider the first part in the 2-loop case. 2-loop Feynman graphs for electron's AMM are showed on Figure 2. We must prove that the application of this subtraction procedure is equivalent to the on-shell renormalization. The on-shell renormalization can be represented in the form that is similar to the one that was used for description of the subtraction procedure in Section 2.2, see Table 1. Here,  $B$  is the operator that is applied to Feynman amplitudes of electron self-energy subgraphs for the on-shell renormalization. This operator is defined by the following relation:

$$B\Sigma(p) = \Sigma(m) + (\hat{p} - m)(b(m^2) + 2a'(m^2) + 2mb'(m^2)) \quad (18)$$

if (6) is satisfied<sup>10</sup>.

---

<sup>10</sup>By definition,  $\Sigma(m) = a(m^2) + mb(m^2)$ .

Table 1: Operator expressions for contributions of graphs from Figure 2 to electrons's AMM that are obtained directly by on-shell renormalization, the differences between these expressions and expressions from Table 2.

#	operator expression	difference
1	$A_G - A_G L_{abc}$	$(L_G - U_G)A_{abc} - A_G(L_{abc} - U_{abc})$
2	$A_G$	0
3	$A_G - A_G L_{bcd}$	$A_G(U_{abc} - L_{abc})$
4	$A_G - A_G L_{bcd}$	$A_G(U_{abc} - L_{abc})$
5	$A_G - A_G B_{bc}$	$A_G(U_{bc} - B_{bc})$
6	$A_G - A_G B_{bc}$	$A_G(U_{bc} - B_{bc})$
7	$A_G - A_G U_{de}$	0

As shown in this table, the contribution of the graph 1 to  $a_{e,1} - a_{e,1}^{new}$  is equal to zero. Let us consider the contribution of graphs 3–6 to this difference. Note that the following statement is valid. Suppose the functions  $\Sigma(p)$ ,  $\Gamma_\mu(p, q)$  and the complex number  $C$  satisfy the following conditions:

- (6), (7);
- the Ward identity:

$$\Gamma_\mu(p, 0) = -\frac{\partial \Sigma(p)}{\partial p^\mu};$$

- $U\Gamma_\mu = C\gamma_\mu$ ;

then  $U\Sigma(p) = \Sigma(m) - C(\hat{p} - m)$ . Also, if additionally  $(U - L)\Gamma_\mu = C_1\gamma_\mu$ , then  $(U - B)\Sigma(p) = -C_1(\hat{p} - m)$ . From this it follows that the contribution of graphs 3–6 is equal to zero. The complete proof of the relation  $a_{e,1}^{new} = a_{e,1}$  for any order of perturbation will be given elsewhere [40].

Let us consider the elimination of divergences in the 2-loop case. Note that overall UV-divergences are removed by the operator  $A$ , see [44]. Thus, graph 2 doesn't have divergences, all UV-divergences in graph 7 are obviously removed. Also, some subgraphs can generate IR-divergences, see [44]. The vertex that is incident to the external photon line is a such subgraph in graphs 1–6. However, these IR-divergences ("overall") are removed by operator  $A$ , see [44]. Each of graphs 3–6 has a unique UV-divergent subgraph that doesn't coincide with the whole graph. The UV-divergence corresponding to this subgraph is subtracted by the counterterm with operator  $U$ . However, operator  $U$  doesn't generate additional IR-divergences (in contrast to operators  $L$  and  $B$ ) because all IR-divergences in Feynman amplitudes like (7)

are proportional to  $p_\mu$  or  $\hat{p}p_\mu$ , all IR-divergences in (18) are contained in terms with  $a'(m^2)$  or  $b'(m^2)$ . In the graph 1 the subgraph  $abc$  generates UV and IR divergences simultaneously. The UV-divergence that corresponds to  $abc$  is subtracted by the counterterm  $A_G U_{abc}$ , this counterterm doesn't generate additional IR-divergences. The IR-divergence that corresponds to the subgraph  $abc$  is subtracted by the counterterm  $(L_G - U_G)A_{abc}f_G$ . This counterterm doesn't generate additional UV-divergences. In this cases all divergences are eliminated point-by-point, before integration<sup>11</sup>. The point-by-point elimination of divergences will be described in detail elsewhere [40].

## 4 Application of the method to computation of $A_1^{(4)}$ and $A_1^{(6)}$

The described above method of divergence elimination was applied to the computation of 2-loop and 3-loop corrections to the electron AMM. The purpose of this calculation is to check the subtraction procedure. The D programming language [46] was used. The code for the integrands was generated automatically in the C programming language. The Feynman gauge (4) and the following values of the constants:  $C_A = 0$  from (5) and  $C_U = 0$  from (8) were used. The numerical integration was performed by an adaptive Monte Carlo method. Each Feynman graph was computed separately. Feynman graphs that are obtained from each other by changing the direction of electron lines were computed separately. The integration domain was split into 620 and 5100 subdomains for computation of  $A_1^{(4)}$  and  $A_1^{(6)}$  respectively. The following probability density function for Monte Carlo integration was used:

$$C_{j(\underline{z})} \frac{\min(z_1, \dots, z_n)^s}{z_1 \dots z_n},$$

where  $s \approx 0.74$ ,  $j(\underline{z})$  is the number of the subdomain containing the tuple  $\underline{z} = (z_1, \dots, z_n)$ , coefficients  $C_j$  were adjusted dynamically. The splitting of the integration domain into subdomains is performed by the following rules:

- For each tuple  $\underline{z}$  we determine a partition of the set of indexes of  $\underline{z}$  into two non-empty subsets  $A$  and  $B$  such that  $(\min_B z_l)/(\max_A z_l)$  is maximal. So, the integration domain is split into  $2^n - 2$  pieces.

---

<sup>11</sup>As was noted above, the application of the given subtraction procedure for graph 1 is equivalent to the on-shell renormalization. However, this equivalence is not point-by-point in the Feynman-parametric representation. In particular, the on-shell renormalization doesn't lead to a convergent integral for graph 1.

- Each piece is split into 10 parts. The number of a part for the tuple  $\underline{z}$  is the number of interval from the list

$$[0; 1], (1; 2], (2; 3], (3, 5], (5, 7],$$

$$(7, 10], (10, 14], (14, 18], (18, 22], (22, +\infty),$$

that contains the value  $\ln((\min_B z_l)/(\max_A z_l))$ .

The integrand appears as a difference of functions such that the corresponding integrals can diverge. Moreover, these divergences can have a linear character or even more. Thus, round-off errors can introduce a significant contribution to the result. In the cases when the 64-bit precision was not enough, we used the 320-bit precision (with the help of the SCSLib library [47]). These situations appear with the probability of about 1/2000 during the Monte Carlo integration. The situations when the 320-bit precision is not enough appear with the probability less than  $10^{-9}$  and don't introduce any noticeable contribution (these points are discarded).

3 days of computation on a personal computer give the following result:

$$A_1^{(4)} = -0.328513(87),$$

$$A_1^{(6)} = 1.1802(85)$$

(the uncertainties hereinafter represent the 90% confidential limits). These results are in good agreement with (2), (3). The uncertainties are due to the statistical error of the Monte Carlo integration. These uncertainties can be made arbitrarily small by increasing the time of computation.

7 Feynman graphs contributing to  $A_1^{(4)}$  are showed on Figure 2, contributions of each graph to  $A_1^{(4)}$  are presented in Table 2. In this table and in the following tables the number  $N_{\text{call}}$  denotes the number of function calls during the numerical integration. The calculated contribution of graphs 1, 2, and 7 are in good agreement with well-known values that were obtained from analytical expressions (0.77747802,  $-0.46764545$ , and 0.01568742, respectively), see [13, 14, 16].

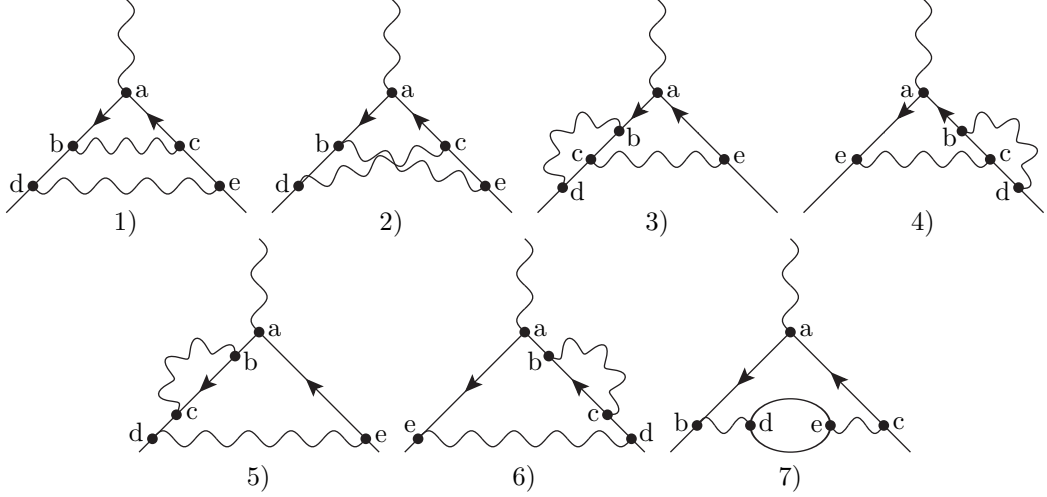


Figure 2: 2-loop Feynman graphs for electron's AMM.

Table 2: Contributions of graphs from Figure 2 to  $A_1^{(4)}$  with operator expressions from which these contributions are obtained.

#	value	$N_{\text{call}}$	operator expression
1	0.777455(52)	$5 \cdot 10^9$	$A_G - A_G U_{abc} - (L_G - U_G) A_{abc}$
2	-0.467626(44)	$4 \cdot 10^9$	$A_G$
3	-0.032023(29)	$2 \cdot 10^9$	$A_G - A_G U_{bcd}$
4	-0.032033(29)	$2 \cdot 10^9$	$A_G - A_G U_{bcd}$
5	-0.294978(25)	$2 \cdot 10^9$	$A_G - A_G U_{bc}$
6	-0.294998(24)	$2 \cdot 10^9$	$A_G - A_G U_{bc}$
7	0.0156895(25)	$2 \cdot 10^9$	$A_G - A_G U_{de}$

72 Feynman graphs that contribute to  $A_1^{(6)}$  are shown on Figure 3. The computed contributions of each graph to  $A_1^{(6)}$  are presented in Table 3. Table 4 contains the comparison of the computed contributions of some sets of graphs with known values for these contributions. We selected such sets of graphs that their contributions calculated by the given subtraction procedure is equal (should be equal) to the contributions computed directly in the Feynman gauge. If all computations would be performed with 64-bit precision, the points for which this precision is not enough would be discarded, then it appears an additional error being more than 0.1% in graphs 28, 35–36, 45–46, 70–71.

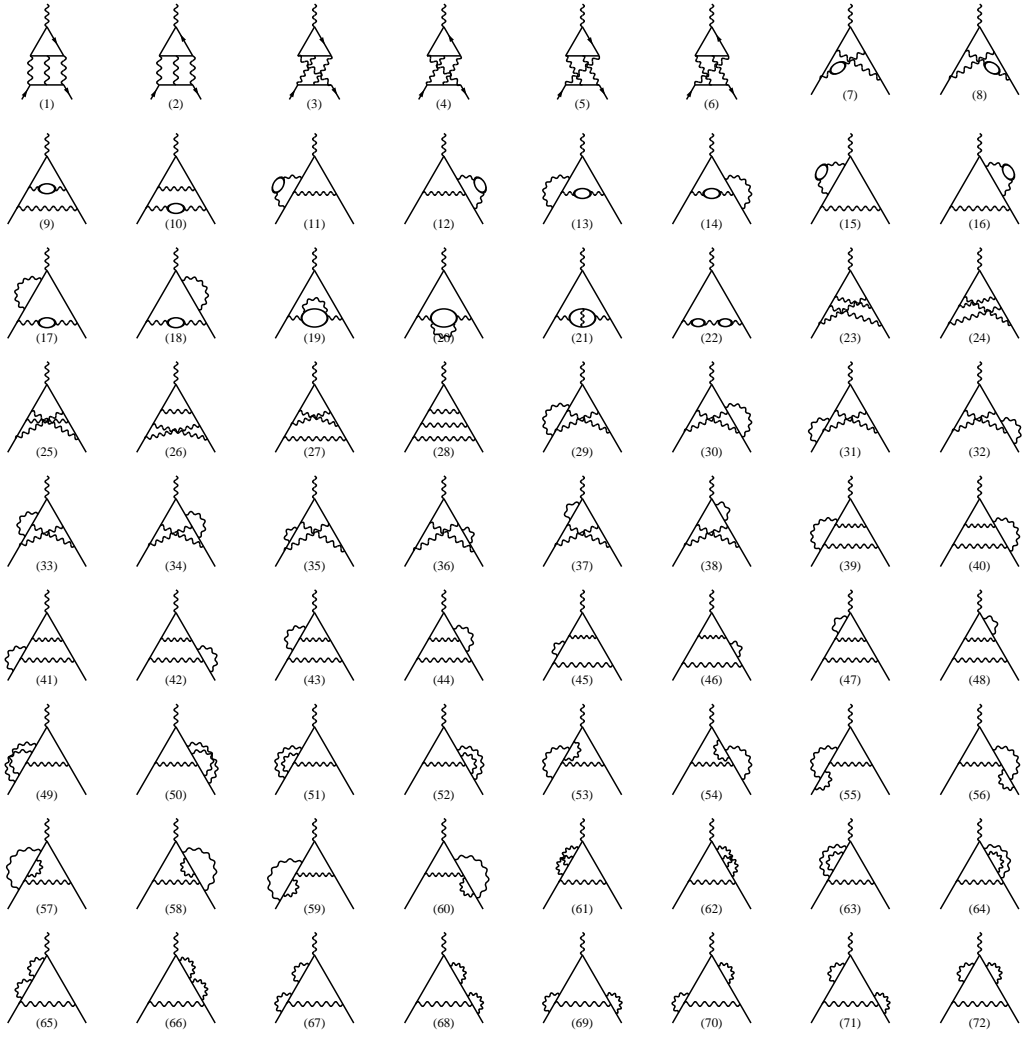


Figure 3: 3-loop Feynman graphs for electron's AMM. Plot courtesy of F. Jegerlehner



Table 3: Contributions of graphs from Figure 3 to  $A_1^{(6)}$ .

#	value	$N_{\text{call}}$	#	value	$N_{\text{call}}$
1	-0.17836(43)	$9 \cdot 10^7$	37	0.15782(86)	$10^8$
2	-0.17862(43)	$9 \cdot 10^7$	38	0.15674(86)	$2 \cdot 10^8$
3	0.18220(61)	$10^8$	39	-0.16718(67)	$10^8$
4	0.18217(61)	$10^8$	40	-0.16750(67)	$10^8$
5	0.18155(61)	$10^8$	41	-1.6283(17)	$3 \cdot 10^8$
6	0.18188(62)	$10^8$	42	-1.6283(17)	$3 \cdot 10^8$
7	-0.042127(73)	$7 \cdot 10^7$	43	0.3054(10)	$2 \cdot 10^8$
8	-0.042245(74)	$7 \cdot 10^7$	44	0.3058(10)	$2 \cdot 10^8$
9	0.11513(16)	$8 \cdot 10^7$	45	2.2553(19)	$4 \cdot 10^8$
10	0.019128(59)	$7 \cdot 10^7$	46	2.2569(18)	$4 \cdot 10^8$
11	0.028301(50)	$7 \cdot 10^7$	47	-1.1357(11)	$2 \cdot 10^8$
12	0.028278(51)	$7 \cdot 10^7$	48	-1.1341(11)	$2 \cdot 10^8$
13	-0.015016(72)	$7 \cdot 10^7$	49	0.10755(42)	$10^8$
14	-0.015153(72)	$7 \cdot 10^7$	50	0.10718(41)	$10^8$
15	-0.072255(92)	$7 \cdot 10^7$	51	-0.01470(38)	$9 \cdot 10^7$
16	-0.072144(93)	$7 \cdot 10^7$	52	-0.01421(38)	$9 \cdot 10^7$
17	-0.041038(94)	$7 \cdot 10^7$	53	0.07232(57)	$10^8$
18	-0.041091(93)	$7 \cdot 10^7$	54	0.07212(56)	$10^8$
19	0.019872(72)	$7 \cdot 10^7$	55	-0.8390(10)	$2 \cdot 10^8$
20	0.019857(71)	$7 \cdot 10^7$	56	-0.8394(10)	$2 \cdot 10^8$
21	0.013153(88)	$7 \cdot 10^7$	57	0.40154(69)	$10^8$
22	0.002548(20)	$6 \cdot 10^7$	58	0.40295(69)	$10^8$
23	0.9311(10)	$2 \cdot 10^8$	59	0.41612(82)	$10^8$
24	0.9318(10)	$2 \cdot 10^8$	60	0.41581(81)	$10^8$
25	-0.02688(47)	$10^8$	61	1.2625(11)	$2 \cdot 10^8$
26	-0.9458(11)	$2 \cdot 10^8$	62	1.2620(11)	$2 \cdot 10^8$
27	-2.2306(19)	$4 \cdot 10^8$	63	-0.02913(63)	$10^8$
28	1.7888(19)	$4 \cdot 10^8$	64	-0.02911(62)	$10^8$
29	-0.87900(74)	$10^8$	65	-1.0614(10)	$2 \cdot 10^8$
30	-0.87894(74)	$10^8$	66	-1.0620(10)	$2 \cdot 10^8$
31	2.5206(17)	$3 \cdot 10^8$	67	-0.04893(73)	$10^8$
32	2.5207(17)	$3 \cdot 10^8$	68	-0.04831(72)	$10^8$
33	0.07018(50)	$10^8$	69	-2.9084(20)	$4 \cdot 10^8$
34	0.07017(50)	$10^8$	70	3.2668(21)	$5 \cdot 10^8$
35	-1.7479(16)	$3 \cdot 10^8$	71	3.2652(21)	$4 \cdot 10^8$
36	-1.7498(16)	$3 \cdot 10^8$	72	-3.2047(20)	$4 \cdot 10^8$

Table 4: Comparison of contributions of some sets of Feynman graphs from Figure 3 to  $A_1^{(6)}$  with known analytical values.

#	value	analyt. value	Ref.
1–6	0.3708(14)	0.3710052921	[31]
7–10	0.04989(20)	0.05015	[25, 26] <sup>a</sup>
11–12,15–16	−0.08782(15)	−0.0879847	[23, 25]
13–14,17–18	−0.11230(17)	−0.112336	[24, 25]
19–21	0.05288(13)	0.05287	[22]
22	0.002548(20)	0.0025585	[22]
23–24	1.8629(14)	1.861907872591	[32]
25	−0.02688(47)	−0.026799490	[33]
26–27	−3.1764(22)	−3.17668477	[29]
28	1.7888(19)	1.79027778	[29]
29–30	−1.7579(10)	−1.757936342	[33]
31–32,37–38	5.3559(27)	5.35763265	[29, 30]
33–34,37–38	0.4549(14)	0.45545185	[29, 32]
31–32,35–36	1.5436(34)	1.541649	[28, 30]
33–36	−3.3573(24)	−3.360532	[28, 32]
39–40	−0.33468(95)	−0.334695103723	[32]
41–48	−0.4030(41)	−0.4029	[27, 28]
49–72	0.9529(53)	0.9541	[27–30, 32, 33]

<sup>a</sup> There is a disagreement of contributions of sets 7–8 and 9–10 separately with values that are given in that papers. We failed to find the reason, but the contribution of 7–10 is in good agreement, the error is less than 0.6%.

## 5 Acknowledgments

I am grateful to A.L. Kataev for many useful discussions and recommendations, help in organizational issues, to O.V. Teryaev for helpful discussions and help in organizational issues, to L.V. Kalinovskaya for help in organizational issues, to A.B. Arbuzov for help in preparing this version of the text and help in organizational issues.

This research was partially supported by RFBR Grant N 14-01-00647.

## References

- [1] N.N. Bogoliubov, O.S. Parasiuk // Acta Math. 97, 227 (1957).

- [2] K. Hepp Proof of the Bogoliubov-Parasiuk Theorem on Renormalization // Commun. math. Phys. — 1966. — V.2. — 301–326.
- [3] V.A. Scherbina // Catalogue of Deposited Papers, VINITI, Moscow, 38, 1964 (in Russian).
- [4] O.I. Zavialov, B.M. Stepanov // Yadernaja Fysika (Nuclear Physics) 1, 922, 1965 (in Russian).
- [5] W. Zimmermann, Convergence of Bogoliubov’s Method of Renormalization in Momentum Space // Commun. math. Phys. — 1969. — V. 15. — 208–234.
- [6] V.B. Berestetskii, E.M. Lifshitz, L.P. Pitaevskii, Quantum Electrodynamics, Butterworth-Heinemann, 1982.
- [7] N.N. Bogoliubov, D.V. Shirkov, Introduction to the Theory of Quantized Fields, John Wiley & Sons Inc, 1980.
- [8] D. Hanneke, S. Fogwell Hoogerheide, G. Gabrielse, Cavity control of a single-electron quantum cyclotron: Measuring the electron magnetic moment // Physical Review A. — 2011. — V. 83, 052122.
- [9] T. Aoyama, M. Hayakawa, T. Kinoshita, M. Nio, Tenth-Order QED Contribution to the Electron  $g - 2$  and an Improved Value of the Fine Structure Constant // Physical Review Letters — 2012. — V. 109, 111807.
- [10] T. Aoyama, M. Hayakawa, T. Kinoshita, M. Nio, Tenth-Order Electron Anomalous Magnetic Moment – Contribution of Diagrams without Closed Lepton Loops // Physical Review D. — 2015. — V. 91, 033006.
- [11] J. Schwinger, On Quantum Electrodynamics and the magnetic moment of the electron // Physical Review. — 1948. — V. 73. — 416.
- [12] J. Schwinger, Quantum Electrodynamics, III: the electromagnetic properties of the electron — radiative corrections to scattering // Physical Review. — 1949. — V. 76. — 790.
- [13] R. Karplus, N. Kroll, Fourth-order corrections in Quantum Electrodynamics and the magnetic moment of the electron // Physical Review. — 1950. — V. 77, N. 4. — 536–549.
- [14] A. Petermann, Fourth order magnetic moment of the electron // Helvetica Physica Acta. — 1957. — V. 30. — 407–408.

- [15] C. Sommerfield, Magnetic dipole moment of the electron // Physical Review. — 1957. — N. 107. — 328–329.
- [16] M.V. Terentiev // Soviet Physics JETP, 16, 444 (1963).
- [17] M. Levine, J. Wright, Anomalous magnetic moment of the electron // Physical Review D. — 1973. — V. 8, N. 9. — 3171–3180.
- [18] R. Carroll, Y. Yao,  $\alpha^3$  contributions to the anomalous magnetic moment of an electron in the mass-operator formalism // Physics Letters. — 1974. — V. 48B, N. 2. — 125–127.
- [19] R. Carroll, Mass-operator calculation of the electron  $g$  factor // Physical Review D. — 1975. — V. 12, N. 8. — 2344–2355.
- [20] P. Cvitanović, T. Kinoshita, Sixth-order magnetic moment of the electron // Physical Review D. — 1974. — V. 10, N. 12. — pp. 4007–4031.
- [21] T. Kinoshita, New Value of the  $\alpha^3$  electron anomalous magnetic moment // Physical Review Letters. — 1995. — V. 75, N. 26. — 4728–4731.
- [22] J. Mignaco, E. Remiddi, Fourth-order vacuum polarization contribution to the sixth-order electron magnetic moment // IL Nuovo Cimento. — 1969. — V. LX A, N. 4. — 519–529.
- [23] R. Barbieri, M. Caffo, E. Remiddi, A contribution to sixth-order electron and muon anomalies. – II // Lettere al Nuovo Cimento. — 1972. – V. 5, N. 11. — 769–773.
- [24] D. Billi, M. Caffo, E. Remiddi, A Contribution to the sixth-Order electron and muon Anomalies // Lettere al Nuovo Cimento. — 1972. — V. 4, N. 14. — 657–660.
- [25] R. Barbieri, E. Remiddi, Sixth order electron and muon  $(g - 2)/2$  from second order vacuum polarization insertion // Physics Letters. — 1974. — V. 49B, N. 5. — 468–470.
- [26] R. Barbieri, M. Caffo, E. Remiddi, A contribution to sixth-order electron and muon anomalies – III // Ref.TH.1802-CERN. — 1974.
- [27] M. Levine, R. Roskies, Hyperspherical approach to quantum electrodynamics: sixth-order magnetic moment // Physical Review D. — 1974. — V. 9, N. 2. — 421–429.

- [28] M. Levine, R. Perisho, R. Roskies, Analytic contributions to the  $g$  factor of the electron // Physical Review D. — 1976. — V. 13, N. 4. — 997–1002.
- [29] R. Barbieri, M. Caffo, E. Remiddi, S. Turrini, D. Oury, The anomalous magnetic moment of the electron in QED: some more sixth order contributions in the dispersive approach // Nuclear Physics B. — 1978. — N. 144. — 329–348.
- [30] M. Levine, E. Remiddi, R. Roskies, Analytic contributions to the  $g$  factor of the electron in sixth order // Physical Review D. — 1979. — V. 20, N. 8. — 2068–2077.
- [31] S. Laporta, E. Remiddi, The analytic value of the light-light vertex graph contributions to the electron  $g - 2$  in QED // Physics Letters B. — 1991. — N. 265. — 182–184.
- [32] S. Laporta, The analytical value of the corner-ladder graphs contribution to the electron  $(g - 2)$  in QED // Physics Letters B. — 1995. — N. 343. — 421–426.
- [33] S. Laporta, E. Remiddi, The Analytical value of the electron  $(g-2)$  at order  $\alpha^3$  in QED // Physical Letters B. — 1996. — V. 379. — 283–291.
- [34] T. Kinoshita, W. Lindquist, Eighth-order anomalous magnetic moment of the electron // Physical Review Letters. — 1981. — V. 47, N. 22. — 1573–1576.
- [35] T. Aoyama, M. Hayakawa, T. Kinoshita, M. Nio, N. Watanabe, Eighth-order vacuum-polarization function formed by two light-by-light-scattering diagrams and its contribution to the tenth-order electron  $g-2$  // Physical Review D. — 2008. — N. 78., 053005.
- [36] R. Bouchendira, P. Cladé, S. Guellati-Khélifa, F. Nez, F. Biraben, New Determination of the Fine Structure Constant and Test of the Quantum Electrodynamics // Physical Review Letters. — 2011. — V. 106, 080801.
- [37] P. Mohr, B. Taylor, D. Newell, CODATA recommended values of the fundamental physical constants: 2010\* // Reviews of Modern Physics. — 2012. — V.84, 1527.
- [38] A.L. Kataev, Analytical eighth-order light-by-light QED contributions from leptons with heavier masses to the anomalous magnetic moment of the electron // Physical Review D. — 2012. — N. 86, 013010.

- [39] A. Kurz, T. Liu, P. Marquard, M. Steinhauser, Anomalous magnetic moment with heavy virtual leptons // Nuclear Physics B. — 2014. — V. 879. — 1–18.
- [40] An extended description of the method, in preparation.
- [41] O.I. Zavialov, Renormalized Quantum Field Theory, Springer Science & Business Media, 2012.
- [42] V.A. Smirnov, Renormalization and Asymptotic Expansions, PPH'14 (Progress in Mathematical Physics), Birkhäuser, 2000.
- [43] P. Cvitanović, T. Kinoshita, Feynman-Dyson rules in parametric space // Physical Review D. — 1974. — V. 10, N. 12. — pp. 3978–3991.
- [44] P. Cvitanović, T. Kinoshita, New approach to the separation of ultraviolet and infrared divergences of Feynman-parametric integrals // Physical Review D. — 1974. — V. 10, N. 12. — pp. 3991–4006.
- [45] T. Aoyama, M. Hayakawa, T. Kinoshita, M. Nio, Automated calculation scheme for  $\alpha^n$  contributions of QED to lepton g-2: Generating renormalized amplitudes for diagrams without lepton loops // Nuclear Physics B. — 2006. — V. 740. — pp. 138–180.
- [46] A. Alexandrescu, The D Programming Language, Addison-Wesley Professional, 2010.
- [47] D. Defour, F. Dinechin, Software Carry-Save for fast multiple-precision algorithms // Proceedings of the First International Congress of Mathematical Software, Beijing, China, 2002.